JOURNAL OF MATERIALS SCIENCE 25 (1990) 3765–3772

Microstructure and microchemistry of the Al/SiC interface

S. D. PETEVES, P. TAMBUYSER, P. HELBACH
Institute of Advanced Materials, CEC, PO Box 2, 1755 ZG Petten, The Netherlands
M. AUDIER, V. LAURENT, D. CHATAIN
LTPCM, LA 29 CNRS, ENSEEG, Domaine Universitaire, BP 75, 38042 Saint Martin d'Heres Cedex, France

The characteristics of the Al/SiC interface play a critical role in controlling the properties of SiC-reinforced aluminium composites and aluminium-brazed SiC ceramic joints. Recently, a detailed investigation on the wettability of SiC single crystals by aluminium and several of its alloys was conducted. In order to understand further the nature of the Al/SiC interface, high resolution and conventional transmission electron microscope techniques have now been used to investigate its microchemistry and microstructure. The results revealed the coexistence of two polytype structures, rhombohedral and hexagonal, in the SiC single crystal structure. Aluminium carbide (Al_4C_3) and silicon were the reaction products found at the Al/SiC interface. From diffraction patterns, epitaxial orientation relationships between the SiC substrate and Al_4C_3, Si were determined.

1. Introduction

Ceramic–metal interfaces are of immense growing importance in todays advanced materials technology. As such, for example, the Al/SiC interface is of basic concern in the properties of SiC-joined components and SiC-reinforced aluminium composites, which are prime candidates for use in the automobile and aerospace industry and the first wall of fusion reactors. Some studies on the interfacial structure of the Al/SiC bond have been reported; these are briefly discussed. Even so, as it will be realized, there is limited, if not sometimes contradictory, information on the nature and reactions at the aluminium/silicon carbide interface.

The fracture surface of an Al/SiC composite has been examined in a scanning Auger microprobe (SAM) [1]. The results obtained excluded the formation of Al_4C_3 at the interface, but indicated aluminium diffusion into SiC whereas no silicon had penetrated in the aluminium matrix. No reaction was found on fracture surfaces of Silag SiC/Al also examined in SAM, but instead Al_2O_3 was identified to be present at a few interfaces during transmission electron microscopy (TEM) examination [2]. No evidence of reaction between Al (6061) and the SiC coating of B fibres was found by TEM, but intimate contact at the SiC/Al interface was reported [3]. Indeed the chemical stability of SiC in contact with molten aluminium at temperatures well above the melting temperature of the metal has been suggested [4]. However, in another TEM study [5] of the (A-1050) Al/SiC fibre-reinforced material, precipitation of Al_4C_3 was identified.

Interfaces in SiC whisker-reinforced aluminium alloys fabricated by powder metallurgy methods, were also characterized by the presence of second-phase particles, including oxide and intermetallic phases mainly of the alloy impurities (magnesium, manganese, copper) [6]. In a study of joining SiC with aluminium as interlayer metal [7, 8] the interfacial reactions between both pressureless sintered (PLS) and reaction-bonded (RB) SiC with aluminium have been investigated, after realizing that the fracture strength of the PLS-SiC joints was almost double that of the RB-SiC joints. The TEM study revealed that the Al_4C_3 phase had only formed at the PLS-SiC/Al interface; the existence of free silicon in the RB-SiC had suppressed the formation of the carbide, which was considered to be the major strengthening mechanism of the Al/SiC joint.

Another study of joining PLS-SiC ceramics [9] with an Al/Ti/Al insert foil showed that the only aluminium phases formed at the interface were those of $TiAl_3$(Si) and Al_2O_3. Finally, recent thermodynamic studies [10, 11] of the Al–SiC system explained the formation of Al_4C_3 at the interface, and revealed the effects of impurities or alloying elements in aluminium on the nature of the Al/SiC interface. Interestingly enough it was concluded that although Al_4C_3 may not always precipitate, the SiC surface would anyway be modified on contact with aluminium. There exists also a theoretical study which attempting to explain the SiC/Al interface bond from an atomic viewpoint [12]. The conclusion drawn from this study, which assumes a clean interface, is that the adhesion is large for the interface between Al(1 1 1) and α-SiC(0 0 0 1) only if the Al(1 1 1) plane is reconstructed (i.e. with dislocations).

This study is a continuation of an earlier investigation

0022–2461/90 $03.00 + .12

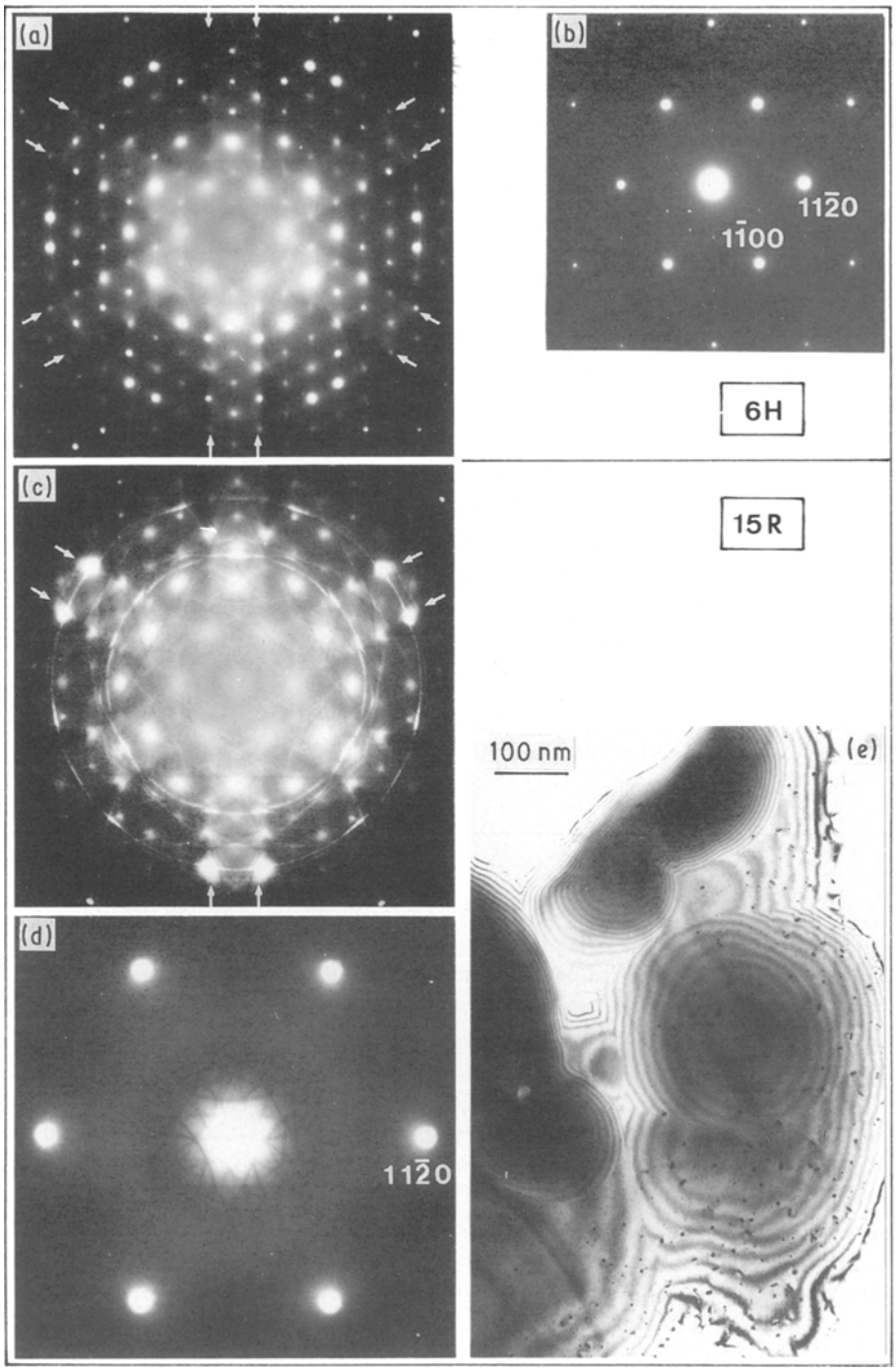

Figure 1 The SiC single-crystal structures: (a) CBED pattern showing a six-fold symmetry of hexagonal SiC polytype; (b) corresponding SAED pattern showing $1\bar{1}00$ spots characteristic of hexagonal polytype structures; (c) CEBD pattern showing a three-fold symmetry of either cubic or rhombohedral structure SiC polytype; (d) corresponding Kikuchi line pattern; (e) bright-field image of the SiC substrate exhibiting equal thickness fringes.

[13, 14] on the wettability of SiC single crystals by aluminium and its alloys in the temperature range 700 to 900° C, and under such experimental conditions that allowed the formation of a true metal(alloy)/SiC interface. In the Al/SiC system, a non-wetting to wetting transition was observed at a temperature that decreased as the time increased. The onset of the transition was attributed to the dissolution of SiC into aluminium rather than the formation of Al_4C_3 at the interface. The latter was verified by observing the same wetting behaviour in the Al–Si alloy/SiC system, in which the formation of Al_4C_3 is suppressed by the presence of silicon in aluminium. The aim now is to investigate the nature of the interface between pure aluminium and SiC by verifying and providing insight information on the possible formation of the aluminium carbide.

2. Experimental procedure

Thin foils were prepared from samples consisting of an adhered aluminium drop on the SiC substrate, that had been prepared as discussed in detail elsewhere [13, 14]. Aluminium was of 99.9999% purity and the SiC substrates were of the hexagonal structure single crystals (α-SiC). The SiC platelets were taken from growth clusters of material prepared by the Acheson furnace process. The particular samples examined had been heated to 850° C and held for 60 to 100 min in the range 700 to 800° C under vacuum conditions better than 10^{-5} Pa.

The starting sample was an irregularly shaped platelet of silicon carbide with one flat surface on which a small drop of aluminium (about 2 mm wide and 0.5 mm high) adhered. The aluminium drop was first removed by grinding until only a thin layer

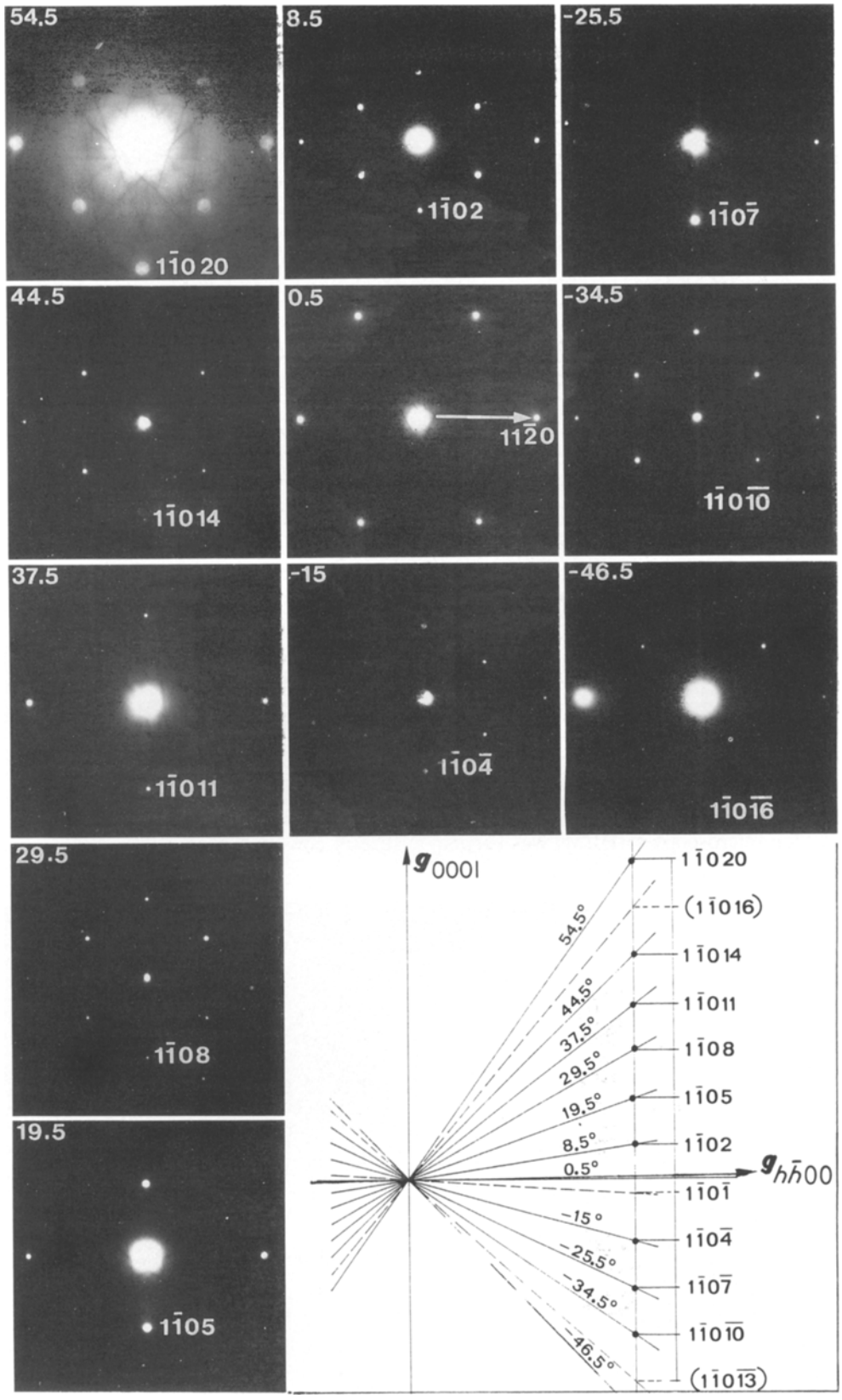

Figure 2 Characterization of the 15R type structure SiC polytype. From systematic tilting (tilt angles are given at the top left side of each SAED pattern) about the 1 1 0 vector the periodic 0 0 0 1 sequence is identified by reporting the magnitude of $1\bar{1}01$ vectors as a function of tilt angle (see diagram at the bottom right corner).

of a few micrometres of aluminium were left on the SiC surface. From the resulting sample a thin (600 μm) slice was cut, which was further thinned down to a thickness of 20 μm by mechanical polishing from the SiC side. Electron-beam transparency was accomplished by 5 kV argon-ion milling. Using this technique, the remaining aluminium film was removed by thinning at an angle of 22° with a gun current of 1 mA. The thinning process continued until all the aluminium was removed from the central area of the specimen. Then the opposite side was thinned down until perforation, by means of a 0.5 mA beam

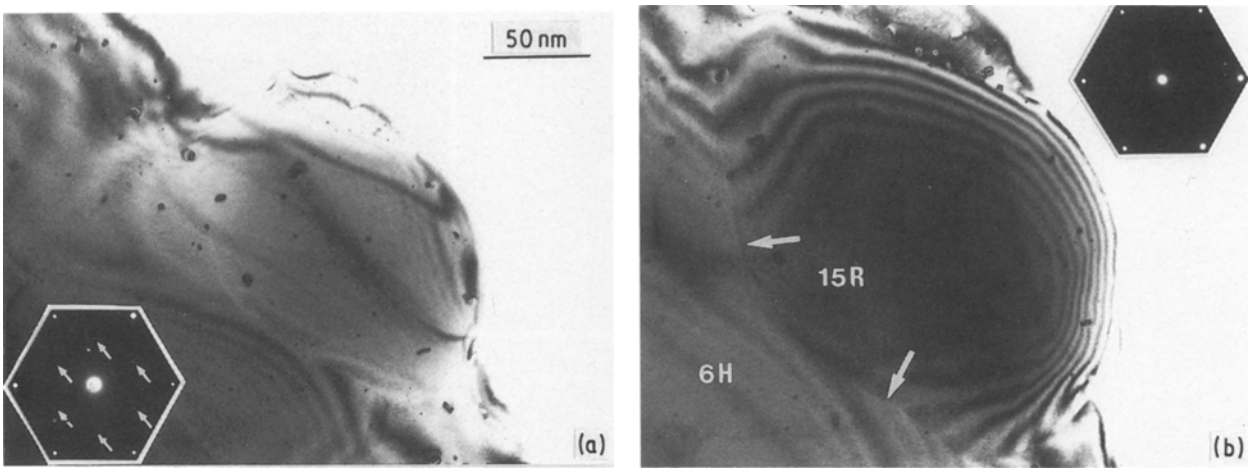

Figure 3 (a) Bright-field image of the SiC substrate and the corresponding diffraction pattern of (0 0 0 1) SiC zone axis. (b) After slight tilting of the specimen the domain at the left edge is identified as 15R-SiC structure according to the corresponding SAED pattern.

contacting the surface at an angle of 16°. By this procedure it was possible to obtain a specimen which showed transparency at the interface.

The thin foil specimens were analysed using a Philips EM 400T operating at 120 kV and a Jeol 200CX (200 kV) transmission electron microscope. For energy dispersive X-ray analytical (EDS) purposes the EM 400T microscope was operated in the STEM mode, in combination with a Tracor 5500 system. For crystallographic analyses, the specimens were mounted on a double tilt holder, whereas for chemical analyses a low background beryllium holder was used. High resolution electron microscopy (HREM) was carried out in the 200CX microscope, equipped with a top entry specimen holder and objective polar pieces of spherical aberration $c_s = 1.2$ mm.

3. Results

3.1. Structure of the SiC single crystal

It has been shown that the long-range structural order of silicon carbide is rather complex as a result of polytypism [15]. The X-ray diffraction spectrum of SiC single crystals, reduced to powder, showed that the main polytype in the samples is of hexagonal structure denoted 6H [16] or (3, 3) [17], i.e. its structure is constituted of a repeated sequence of three

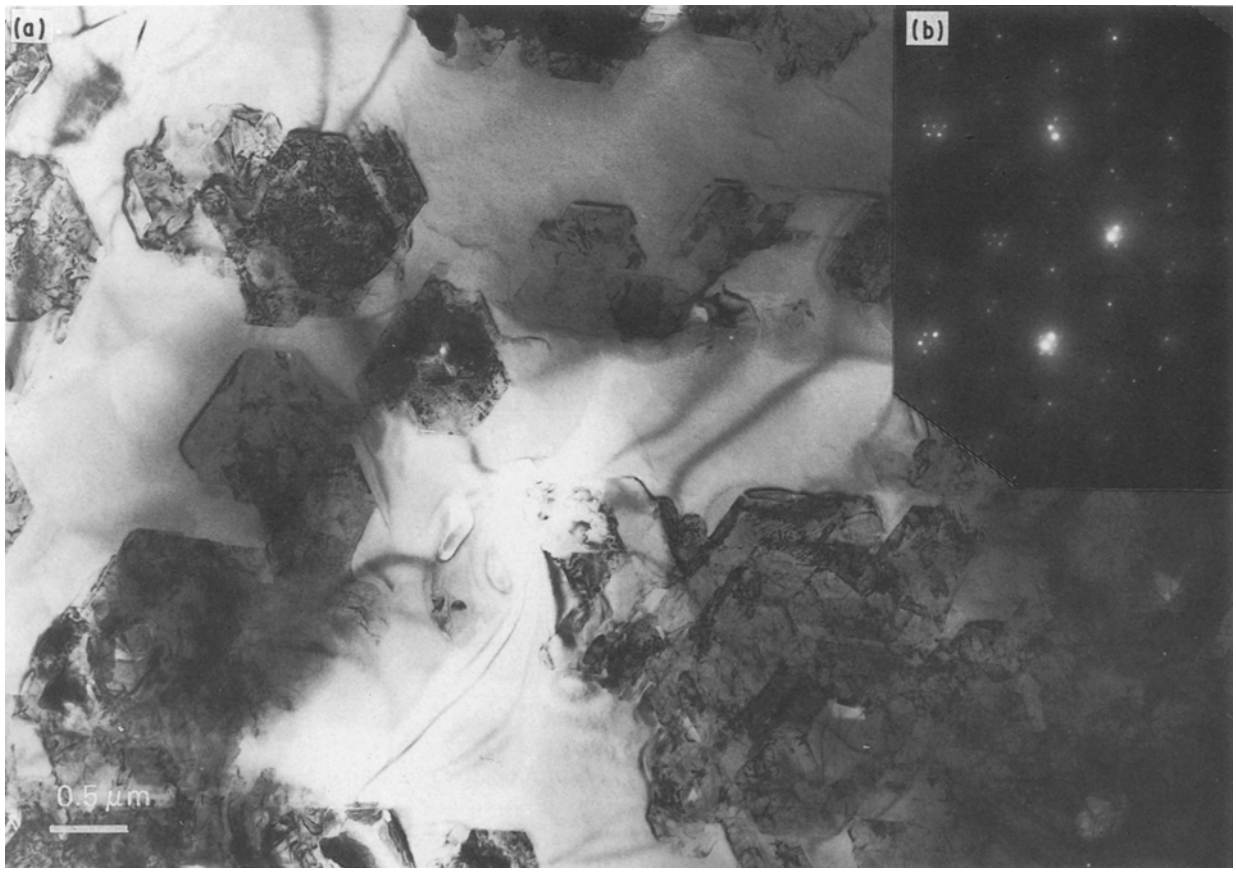

Figure 4 (a) Bright-field image of Al_4C_3 hexagonal crystals on the SiC substrate. (b) The diffraction pattern of one of the Al_4C_3 crystals, with obvious double diffraction spots, presents an orientation relationship with the SiC substrate. (c) An Al_4C_3 crystal outlined with (1 0 $\bar{1}$ 0) facets.

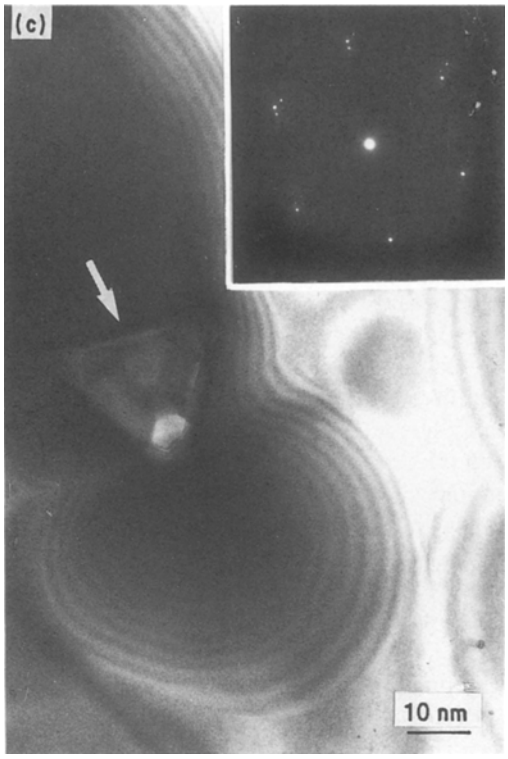

Figure 4 Continued

adjacent parallel and three anti-parallel layers of vertices of connected SiC_4 (or CSi_4) tetrahedra. From a comparison between the calculated 6H spectrum and that experimentally observed, one or several other SiC polytypes have to be expected. However, it is not straightforward to identify these by X-ray diffraction, so TEM techniques were further employed.

The coexistence of different SiC polytypes was first evidenced by convergent beam electron diffraction (CBED) allowing a recognition of the symmetry order of polar axes (Fig. 1): (i) a six-fold axis corresponding to polytypes of the $P6_3mc$ space group, and (ii) a three-fold axis corresponding either to the cubic $F\bar{4}3m$ polytype (β-SiC) or to rhombohedral polytypes of space group R3m [18]. In Figs 1a and b, both of these symmetry order polar axes are distinguished from the different distribution of intensities in the higher order of Laue zone (HOLZ) rings of reflections; the polar axis symmetry order can also be identified from the HOLZ lines pattern observed in the central spot (e.g. Fig. 1d, for a rhombohedral or cubic polytype). In parallel incident beam conditions for diffraction, these two [0 0 0 1] and [1 1 1] zone axes diagrams exhibit different sets of diffracting spots, i.e. $1\bar{1}00$-reflections are permitted for hexagonal polytypes (Fig. 1b) but not for the rhombohedral (or cubic) ones (Fig. 1d). The bright-field image (Fig. 1e) corresponding to these electron diffraction patterns, shows domains defined by circular equal thickness fringes which may be considered as resulting from the coexistence of different SiC polytypes, as discussed later. However, such domains, also observed for a same structure polytype, could indicate a nucleation and growth phenomenon. Further investigations will be necessary to clarify this point.

Two polytypes, 6H and 15R, were identified by electron diffraction from the [0 0 0 1] and [1 1 1] zone

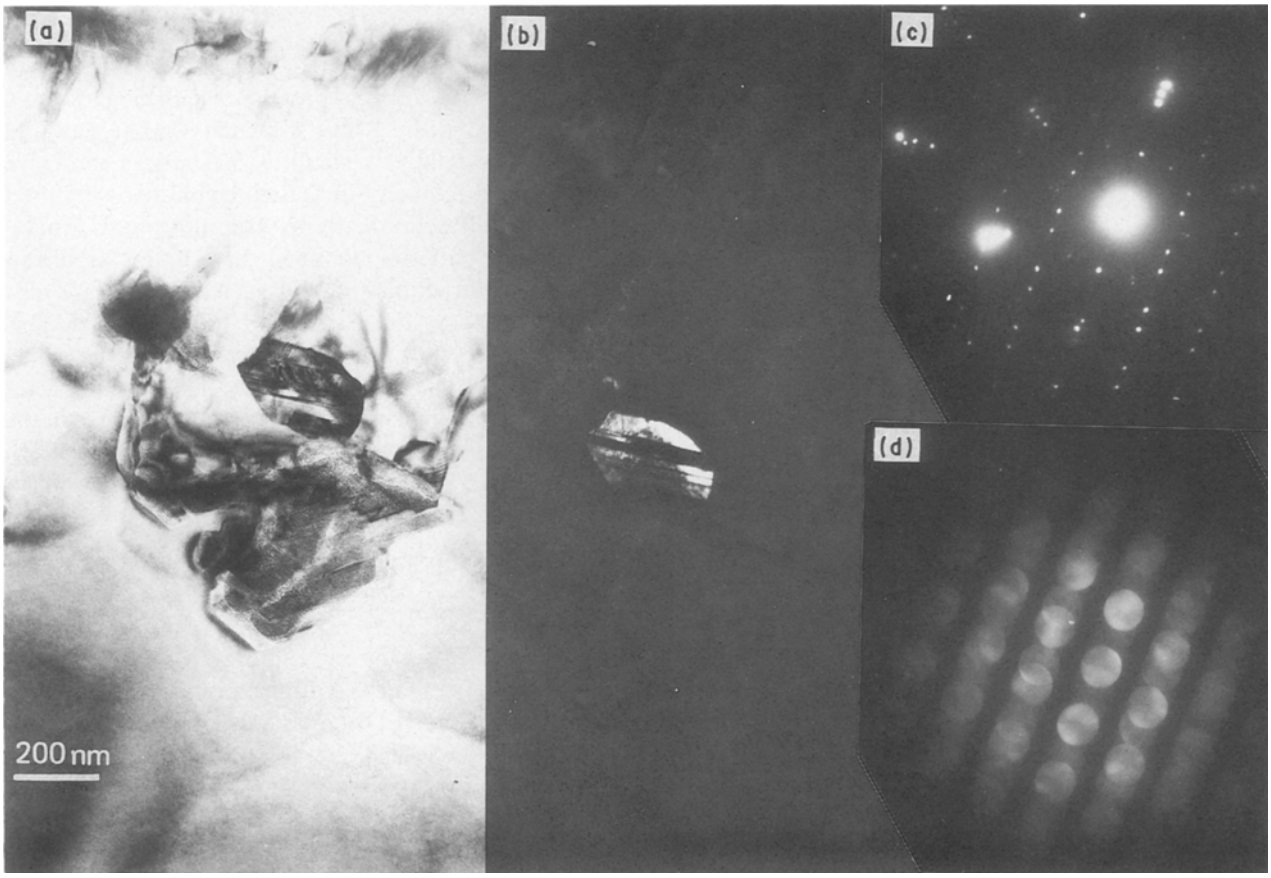

Figure 5 (a) Bright-field image of Al_4C_3 including a silicon crystal. (b) Dark field of the silicon crystal showing twinning. (c) Diffraction pattern with paired spots from the twinned silicon. (d) Microdiffraction pattern of the silicon crystal.

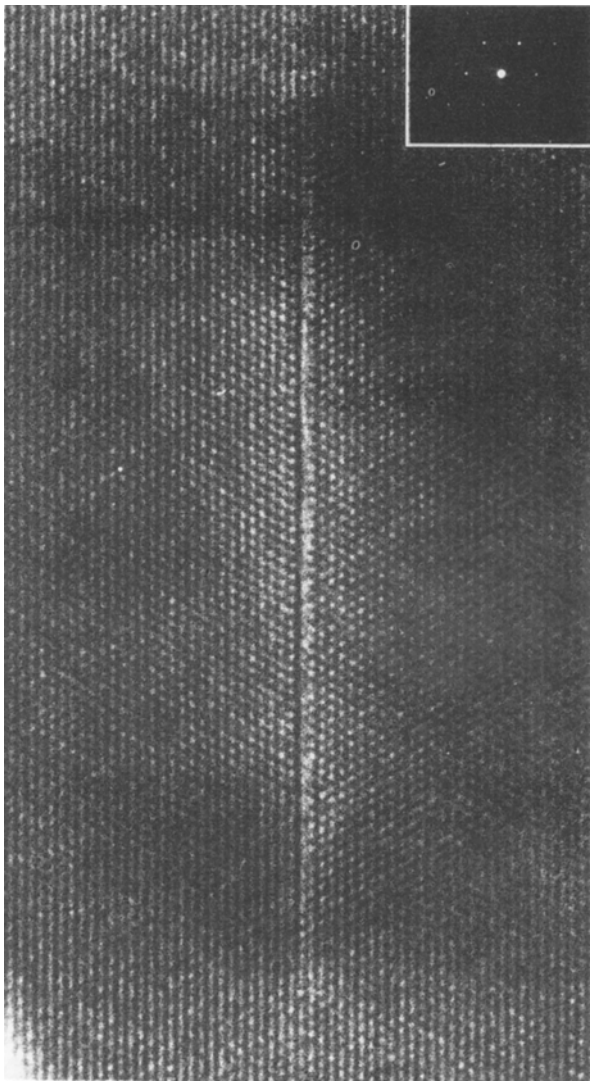

Figure 6 Structural defects observed in the SiC crystal along the (1 $\bar{1}$ 0 1) plane.

axis patterns, which correspond to the average plane of the thin foil; the characterization of the SiC polytypes further requires an identification of the various zone axis patterns resulting from the systematic tilting of a same selected domain area of the sample, with the tilt angles recorded at each photographed zone axis pattern. Following this approach, it is found that indexing of periodic 0 0 0 1 sequences, characteristic of each polytype, is readily possible by reporting, on a diagram, the magnitude of diffracting vector $\boldsymbol{g}_{hkjl}$ (l variable) observed at different tilt angles. The example reported in Fig. 2 concerns the identification of the rhombohedral structure 15R, characterized by a $(3, 2)_3$ layer sequence. Note in Fig. 2 that some diffraction patterns can be confused with those of the cubic (β-SiC) structure, i.e. the pattern observed at 54.5° could also be indexed as a [0 0 1] zone axis in the β-SiC system. In such a case, the absence of β-SiC structure can be ensured by CBED where only one mirror plane is found instead of two.

Further investigations in dark and bright field of the same site of the sample, allowed the localization of the area of coexistence of the polytypes. The interface between the two, 6H and 15R, polytypes shown in Fig. 3 can be obtained when there is a slight misorientation between the polar axes of the two structures. At zero tilt, the ⟨0 0 0 1⟩ orientation of the SiC single crystal was confirmed by means of selected-area diffraction patterns (SAED) taken at different sites of the specimen.

3.2. Al/SiC interface

At the interface on the aluminium side, small crystals having an hexagonal outline or more often aggregates of these crystals were observed, as shown in Fig. 4. The size of these aggregates was of the order of 0.1 to 2 μm. Qualitative EDS analysis showed the presence of aluminium in these crystals. Sets of SAED patterns of such aggregates, taken at different tilt conditions, allowed for a positive identification of these crystals as aluminium carbide (Al_4C_3). The d-spacings perfectly fit the spacings which were calculated using the lattice parameters [19] for hexagonal Al_4C_3 (a = 0.33388 nm, c = 2.4996 nm). An SAED pattern of the aggregate from Fig. 4a recorded at zero tilt is shown in Fig. 4b. Diffraction spots due to the SiC substrate as well as the Al_4C_3 are both present in the pattern. Analysis of the pattern clearly shows the orientation relationship between the matrix and the carbide to be

$$[0\,0\,0\,1]\ \mathrm{SiC} \parallel [0\,0\,0\,1]\ Al_4C_3$$

$$[2\,1\,0]\ \mathrm{SiC} \parallel [2\,1\,0]\ Al_4C_3$$

From the bright-field image of Fig. 4c one may also deduce that the habit planes between the two crystals SiC and Al_4C_3 would be (1 0 $\bar{1}$ 0) SiC ∥ (1 0 $\bar{1}$ 0) Al_4C_3, provided that the aluminium carbide grows "inside" the SiC substrate. Analysis of several of these carbides showed that all crystals and aggregates have the same orientation relationship.

EDS analysis of the Al_4C_3 precipitates also showed the presence of rounded particles which gave rise to a silicon peak in the X-ray spectrum. As these crystal grains were relatively small (< 300 nm) as shown in Figs 5a and b, microdiffraction techniques were used to isolate diffraction patterns from this phase. Analysis of such patterns identified these grains as silicon crystals. Diffraction spots of such a crystal are also shown in the SAED patterns of Figs 5c and d. This particular crystal is twinned according to the spinel law with (1 1 1) as the twin plane; this twinning gives rise to a superimposition of two [1 1 0] zone axes in the diffraction pattern. Analysis of this diffraction pattern also reveals an orientation relation between the silicon and the SiC or Al_4C_3

$$[1\,1\,0]\ \mathrm{Si} \parallel [0\,0\,0\,1]\ Al_4C_3 \quad \text{or} \quad \mathrm{SiC}$$

$$[1\,\bar{1}\,1]\ \mathrm{Si} \parallel [1\,1\,0]\ Al_4C_3 \quad \text{or} \quad \mathrm{SiC}$$

This type of orientation relationship was confirmed for many precipitates. A slight misorientation (3° to 5°) between the [1 1 0] zone axis of silicon and the [0 0 0 1] of Al_4C_3 (or SiC) was systematically observed (Fig. 5).

4. Discussion

The complex long-range order, or polytypism, in SiC has best been explained [15] on the basis of the screw dislocation-assisted crystal growth mechanism [20].

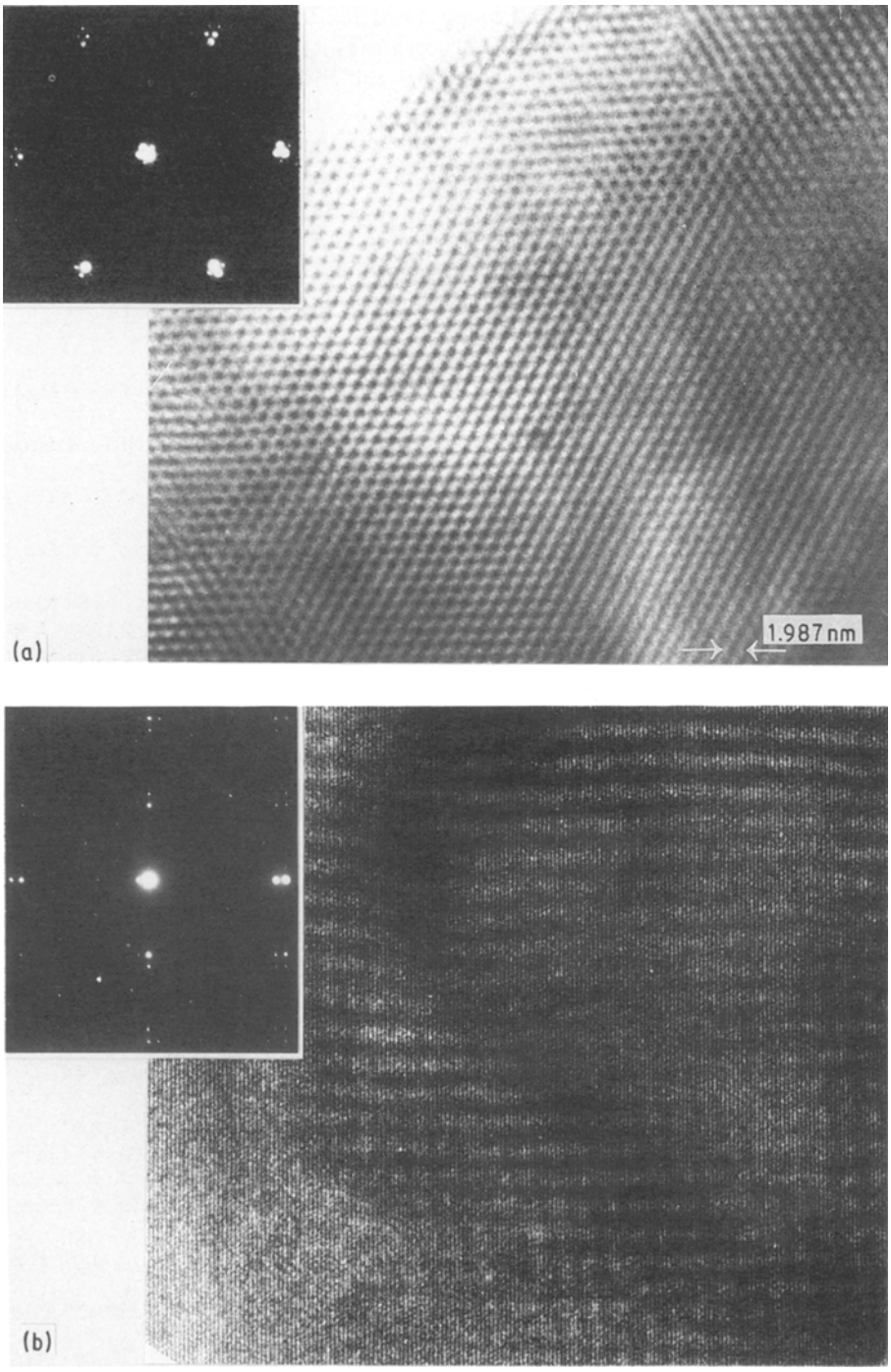

Figure 7 Phenomenon of Moiré fringes due to superposition of Al_4C_3 and SiC phases, for a zone axis of (a) order 3 and (b) order 2, after rotation along the $(1\,1\,\bar{2}\,0)$ type.

Accordingly, structural defects are expected to exist at the interface between two polytypes [17]. However, in the present study there is no such evidence for the 6H/15R-SiC interface as shown in Fig. 3. The only structural defects that could be detected are imperfect dislocations on the $(1\,\bar{1}\,0\,1)$ plane of the SiC phase such as those presented in Fig. 6. It appears that the polytypism in SiC cannot be exclusively explained by a single crystal growth mechanism [15].

The interfacial reaction products between the SiC and aluminium were confirmed to be Al_4C_3 and free silicon. These are expected to form via the reaction

$$3SiC + 4Al \rightarrow Al_4C_3 + 3Si$$

Kinetically the reaction between the aluminium and SiC involves the dissolution of SiC into aluminium, and with increasing carbon activity in it the Al_4C_3 nucleates; this will continue up to a certain level of silicon activity in the Al_l until an equilibrium between $(Al–Si)_l$, SiC and Al_4C_3 is established [10, 11]. At 800° C, for instance, the silicon content in the binary liquid for the equilibrium is about 5 at % [11]. Accordingly, the formation of Al_4C_3, which occurs just below the melting point of aluminium, at 650° C, can be better expressed via the reaction [10]

$$Al_s + SiC \rightarrow Al_4C_3 + (Al–Si)_l$$

From the TEM observations it appears that the aluminium carbide does not grow as a continuous layer on the SiC substrate, which is in agreement with an earlier hypothesis [21] on its formation and growth at the interface of carbon fibre/aluminium. However, it cannot be suggested that Al_4C_3 nucleates at specific sites; it is evident though that several small crystals are formed at an early stage and later these crystals coalesce and form aggregates of Al_4C_3 minute

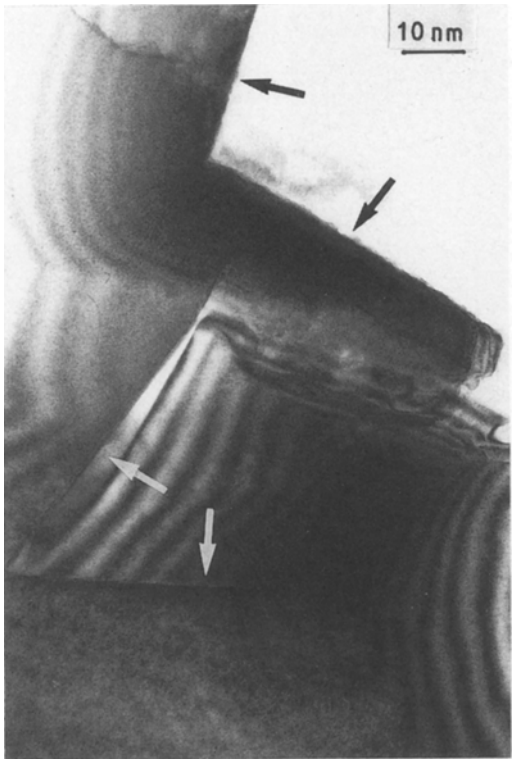

Figure 8 The attack by moisture in the air of Al_4C_3 in the foil results in faceted traces indicatd by arrows in this bright-field image.

precipitates. The free silicon crystals observed as enclosed by the aluminium carbides indicate, as expected, that the (Al–Si) eutectic from which silicon precipitated upon cooling, was "trapped" between grown Al_4C_3 crystals [22]. From EDS analysis, no evidence of aluminium diffusion into the SiC was found. Also, as expected from the low oxygen partial pressures kept during the thermal treatments of the samples, no Al_2O_3 was found at the interface.

In the SiC–Al_4C_3 orientation relationship, the atomic spacing of the $(1\,0\,\bar{1}\,0)$ SiC and Al_4C_3 planes are 0.2691 and 0.2891 nm, respectively, which gives a mismatch of about 8%. However, the interface is without dislocations, as can be deduced from the regular Moiré fringes observed in Figs 7a and b after rotation along the $[1\,1\,\bar{2}\,0]$ type vector. In Fig. 7a, one or two partial dislocations can be pointed out while in Fig. 7b only a rather slight distortion of the interfacial planes is observed. The consistently observed misorientation between the [1 1 0] zone axis of silicon and the [0 0 0 1] of SiC or Al_4C_3, however, rather points to the silicon plane being reconstructed by a dislocation system $\langle 1\,1\,1\rangle$, $\{1\,1\,0\}$.

It is known that the Al_4C_3 tends to react easily with water [8]. A high sensitivity of the carbid to moisture in the air was also experienced in this study. Fig. 8 shows faceted traces of hydrated Al_4C_3 crystals. If the Al/SiC interface, at which Al_4C_3 is present, is considered for use at high temperatures or wet atmospheres, then a barrier between the carbide and the atmosphere will be necessary.

5. Conclusion

The Al/SiC interface, from quenched aluminium sessile drops on SiC single crystals, has been investigated using TEM, STEM and HREM techniques. From the observations it is shown that both SiC crystal polytypes, 6H and 15R, coexist in the structure of the SiC single crystal. The Al/SiC interfacial reaction products were determined to be Al_4C_3 and silicon. Aluminium carbide forms as a discontinuous layer on the SiC substrate, and free silicon precipitates in between the carbide crystals. Simple orientation relationships were found to exist between Al_4C_3, silicon and the SiC substrate.

References

1. R. J. ARSENAULT and C. S. PANDE, *Scripta Metall.* **18** (1984) 1131.
2. H. L. MARKUS, Ann. Tech. Rept., ONRL, Contract N00014-83-K-0143 (1984).
3. K. PREWO and G. McCARTHY, *J. Mater. Sci.* **8** (1972) 919.
4. T. G. NIEH and R. F. KARLAK, *J. Mater. Sci. Lett.* **2** (1983) 119.
5. A. KOHYAMA, N. IGATA, Y. IMAI, H. TERANISHI and T. ISHIKAWA, in "Proceedings of the 5th International Conference on Composite Materials", San Diego, California, 1985, edited by W. C. Harrigan Jr, J. Strife and A. K. Dhingra (TMS-AIME, Warrendale, Pennsylvania, 1986) p. 609.
6. S. R. NUTT, in "Interfaces in Metal Matrix Composites", edited by A. K. Dingra and S. G. Fishman (TMS-AIME, Warrendale, Pennsylvania, 1986) p. 157.
7. T. ISEKI, T. KAMEDA and T. MARUYAMA, *J. Mater. Sci.* **19** (1984) 1692.
8. T. ISEKI, T. MARUYAMA and T. KAMEDA, in "Ceramic Surfaces and Surface Treatment", edited by R. Morell and M. G. Nicholas, British Ceramic Society Proceedings No. 34 (British Ceramic Society, Stoke on Trent, 1984) p. 241.
9. S. MOROZUMI, M. ENDO, M. KIKUCHI and K. ITAMAJIMA, *J. Mater. Sci.* **20** (1985) 3976.
10. K. KANNIKESWARAN and R. Y. LIN, *J. Metals* **9** (1987) 17.
11. J. C. VIALA, P. FORTIER, C. BERNARD and J. BOUIX, in "Proceedings of the 1st European Conference on Composite Materials", edited by A. R. Bunsell, P. Lamicq and A. Massiah (ECCM 1, Bordeaux, France), p. 583.
12. S. LI, R. J. ARSENAULT and P. JENA, *J. Appl. Phys.* **64** (1988) 6246.
13. V. LAURENT, D. CHATAIN and N. EUSTATHOPOULOS, *J. Mater. Sci.* **22** (1987) 244.
14. V. LAURENT, D. CHATAIN, N. EUSTATHOPOULOS and X. DUMANT, in "Cast Reinforced Metal Composites", edited by A. K. Dhingra and S. G. Fishman (ASM International, Metals Park, Ohio, 1988) p. 27.
15. P. T. SCHAFFER, *Acta Crystallogr.* **B25** (1969) 477.
16. Powder Diffraction File, card no. 29-1131 (Joint Committee on Powder Diffraction Standards, Philadelphia, Pennsylvania, 1979).
17. R. S. MITCHELL, *Z. Kristallogr.* **109** (1957) 1.
18. Powder Diffraction File, card no. 22-1301 (Joint Committee on Powder Diffraction Standards, Philadelphia, Pennsylvania, 1979).
19. *Idem*, card no. 35-799.
20. W. K. BURTON, N. CABRERA and F. C. FRANK, *Disc. Faraday Soc.* **5** (1949) 33.
21. S. KOHARA and N. MUTO, in "Proceedings of the 5th International Conference on Composite Materials", San Diego, California, 1985, edited by W. C. Harrigan Jr, J. Stringe and A. K. Dhingra (TMS-AIME, Warrendale, Pennsylvania, 1986) p. 631.
22. V. LAURENT, Thesis INPG, Grenoble, France (1988).

Received 24 April
and accepted 29 September 1989